Article

Epilepsy-Induced High Affinity Blockade of the Cardiac Sodium Current I_{Na} by Lamotrigine; A Potential for Acquired Arrythmias

Juan Antonio Contreras Vite [1], Carlos Vega Valle [2], Happi Biekeu Mbem [1], Sarah-Maude Boivin [1] and Robert Dumaine [1,*]

[1] Department of Pharmacology and Physiology, Faculty of Medicine and Health Sciences, University of Sherbrooke, Sherbrooke, QC J1H 5N4, Canada
[2] Department of Biology, Faculty of Sciences, University of Sherbrooke, Sherbrooke, QC J1K 2R1, Canada
* Correspondence: robert.dumaine@usherbrooke.ca; Tel.: +1-819-821-8000

Abstract: Lamotrigine is widely prescribed to treat bipolar neurological disorder and epilepsy. It exerts its antiepileptic action by blocking voltage-gated sodium channels in neurons. Recently, the US Food and Drug Administration issued a warning on the use of Lamotrigine after observations of conduction anomalies and Brugada syndrome patterns on the electrocardiograms of epileptic patients treated with the drug. Brugada syndrome and conduction disturbance are both associated with alterations of the cardiac sodium current (I_{Na}) kinetics and amplitude. In this study, we used the patch clamp technique on cardiomyocytes from epileptic rats to test the hypothesis that Lamotrigine also blocks I_{Na} in the heart. We found that Lamotrigine inhibited 60% of I_{Na} peak amplitude and reduced cardiac excitability in epileptic rats but had little effect in sham animals. Moreover, Lamotrigine inhibited 67% of I_{NaL} and, more importantly, prolonged the action potential refractory period in epileptic animals. Our results suggest that enhanced affinity of Lamotrigine for I_{Na} may in part explain the clinical phenotypes observed in epileptic patients.

Keywords: ion channels; electrophysiology; patch clamp

1. Introduction

Lamotrigine (Lamictal™, LTG) is an antiepileptic drug approved by the US Food and Drug Administration (FDA) in 1994 to treat bipolar disorders and epilepsy. Part of the antiepileptic action of LTG stems from its ability to block the sodium current [1,2] and possibly the neuronal transient outward potassium current IA [3] expressed in the cortex and hippocampus of the brain. The overall effect is to stabilize the presynaptic membrane of neuronal cells and to attenuate the effect of the excitatory neurotransmitter glutamate during repetitive neuronal firing [4]. Slow binding of LTG during activation or fast inactivation of neuronal sodium channels (nNa_Vs) was proposed to explain the block of sodium current in neurons [2,5–7]. Whether LTG also blocks the cardiac sodium current (I_{Na}) at therapeutic doses (100–500 mg/day) yielding an effective plasma concentration between 2–16 μg/mL (7.8–62.5 μmol/L) [8–10], is unknown. However, clinical observations of Brugada syndrome (BrS) phenotype [11–14] and QRS prolongation [15] on the electrocardiograms (ECG) of epileptic patients treated with LTG are consistent with conduction disturbances and I_{Na} block. Those observations, coupled with a series of case reports on LTG cardiotoxicity [16–18], prompted the FDA to restrict the use of LTG in 2021 and to add a warning label stating that "*Lamictal exhibits class 1B antiarrhythmic activity at therapeutically relevant concentrations.*" [19]. The mechanism by which LTG may exert its arrhythmogenic effect remains unknown. Identifying such potential mechanisms linked to its effect on I_{Na} is the goal of this paper.

In sharp contrast to epileptic patients, studies from toxicology centers indicate that non-epileptic patients on LTG overdose, with serum levels between 17–90 µg/mL, exhibit only minor to moderate neurologic or electrocardiographic effects [18]. This raises the possibility that epilepsy enhances the apparent affinity of LTG for cardiac I_{Na}, possibly by enhancing expression of nNavs in the heart. In support, we previously reported that epilepsy increases the contribution of nNa_Vs to I_{Na} [20,21]. Because of the apparent higher affinity of LTG for neuronal cells, we wanted to test if enhanced expression of nNa_Vs in the heart ventricle may contribute to the arrhythmogenic event clinically reported in epileptic patients.

In this study, we present a series of experiments showing that indeed, epilepsy increased the affinity of LTG for I_{Na}. The enhanced blockade of I_{Na} also prolonged the action potential refractory period. The results may provide a basis to explain the conduction disturbances and the BrS phenotype associated with LTG toxicity in epileptic patients.

2. Results

We first compared the effects of LTG on I_{Na} in ventricular cardiomyocytes from epileptic and sham animals. Figure 1A shows that 10 µmol/L of LTG decreased I_{Na} amplitude more for epileptic animals. Blockade of peak I_{Na} was $16 \pm 6\%$ and $61 \pm 6\%$ for sham and epileptic animals, respectively. Current voltage relationships (Figure 1B) showed that LTG blockade of I_{Na} by 10 µmol/L and 100 µmol/L was similar in epileptic animals. LTG (10 µmol/L) also shifted voltage dependence of I_{Na} activation in epileptic animals but not in sham. Mid-activation voltage ($V_{0.5}$) was depolarized by 5 mV (Table 1, Figure 1C) in cardiomyocytes from epileptic animals. I_{Na} voltage threshold ($I_{Na,Th}$) was depolarized by 5 ± 1 mV and 10.7 ± 1.4 mV with 10 and 100 µmol/L of LTG, respectively, in epileptic animals (Figure 1D), while $I_{Na,Th}$ was depolarized 8.5 ± 1.5 mV by 100 µmol/L of LTG in sham animals. The maximum Na^+ conductance ($G_{Na,max}$) decreased by $49 \pm 5\%$ in the presence of LTG (10 µmol/L) in epileptic animals but had no effect in the sham group (Figure 1E).

Table 1. Na^+ channel activation parameters for control conditions and during exposure to 10 µmol/L of LTG. Tukey test using one-way ANOVA (ctrl vs. LTG), * indicates $p < 0.05$.

Sham	$V_{0.5}$ (mV)	Slope
ctrl	-42 ± 1	4.5 ± 0.2
LTG	-41 ± 1	5 ± 0.2
epileptic		
ctrl	-43 ± 1	4 ± 0.3
LTG	-38 ± 2 *	5.3 ± 0.2 *

2.1. Lamotrigine Blockade of I_{Na}

Our results from Figure 1, showing that blockade of I_{Na} by LTG was larger in epileptic animals, combined with our previous data indicating an increased contribution of TTX-sensitive Na^+ channels [20] during epilepsy, suggest that LTG may target at least two populations of Na^+ channels in ventricular cardiomyocytes. Accordingly, this should translate into a biphasic dose–response curve for I_{Na}. Figure 2A shows that blockade of I_{Na} by LTG in sham animals could be reasonably fit to a single monophasic Hill equation, thus, suggesting that blockade of I_{Na} follows mostly single receptor binding kinetics. In sharp contrast, epileptic rats exhibited a biphasic response to LTG with a high affinity blockade generating a plateau at 47% of the maximum amplitude for concentrations between 10–100 µmol/L and a sensitivity like that of sham animals for larger concentrations. These results indicate at least two LTG binding sites contributed to block I_{Na} during epilepsy. LTG half-maximal blocking concentration (IC_{50}) obtained from the fit to data was 155 ± 22 µmol/L in sham animals. In epileptic conditions, IC_{50} values were 211 ± 48 µmol/L and 1.5 ± 0.3 µmol/L

(Figure 2B). This result, therefore, indicates an increased contribution of LTG-sensitive channels to I_{Na}.
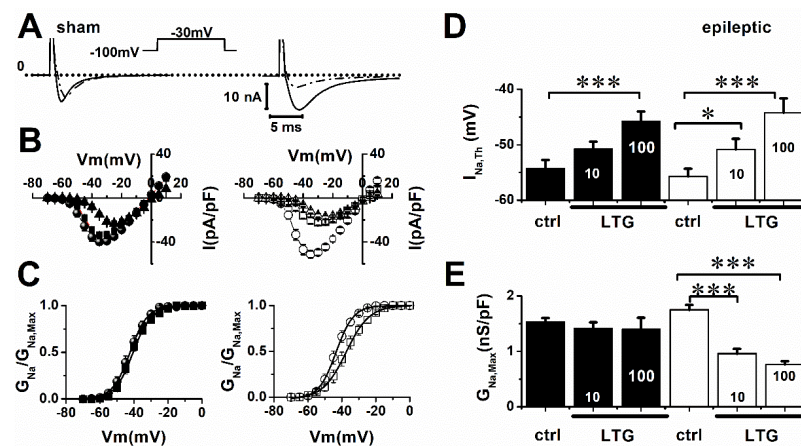

Figure 1. LTG blockade of I_{Na} is increased during epilepsy. (**A**) Inset: voltage clamp protocol. I_{Na} currents were activated by 25 ms voltage steps from −70 to 10 mV, in 5 mV increments, from a −100 mV holding potential. Representative I_{Na} recordings from sham and epileptic rat ventricular cardiomyocytes in control conditions (solid line), and in presence of 10 μmol/L of LTG (dash-dot line). (**B**) Current–voltage relationships (I/V) for sham (filled symbol) and epileptic (open) animals in control conditions (circle), 10 μmol/L (square) and 100 μmol/L of LTG (triangle). (**C**) Normalized I_{Na} activation curves for control and 10 μmol/L of LTG. Data points (±SEM) were fitted to a Boltzmann equation (solid lines). (**D**) LTG (10 μmol/L) depolarized I_{Na} voltage threshold ($I_{Na,Th}$) only in epileptic animals, while 100 μmol/L of LTG significantly depolarized $I_{Na,Th}$ in both groups. Each bar represents average values (±SEM) in control conditions and upon addition of 10 and 100 μmol/L of LTG. (**E**) LTG decreased Na$^+$ channel conductance ($G_{Na,Max}$) in epileptic animals. Average values of $G_{Na,Max}$ in same conditions as (**D**). Tukey test using one-way ANOVA (ctrl vs. LTG), * indicates $p < 0.05$, *** indicates $p < 0.001$. Number of cells: Sham (ctrl, LTG): 13, 14. Epileptic (ctrl, LTG): 14, 13.
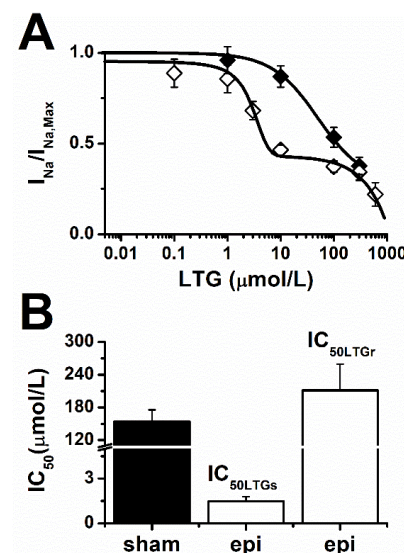
Figure 2. Epilepsy increased the affinity of LTG for I_{Na}. (**A**) Dose response curves for sham (filled symbol) and epileptic (open symbols) animals. The curves were constructed by averaging the ratio between the I_{Na} control value ($I_{Na,Max}$) and its amplitude at each LTG concentration tested. (**B**) IC$_{50}$ values estimated by fitting single- and dual-dose response equations (solid lines) to sham (filled) and epileptic (open) animal data, respectively. Number of cells: Sham (ctrl, LTG): 7–14. Epileptic (ctrl, LTG): 8–13.

2.2. Lamotrigine Prolonged Refractory Period

We next tested if the reduction in I_{Na} caused by LTG could be due to a decrease in Na^+ channel availability (steady-state inactivation). At therapeutic concentration (10 µmol/L), LTG hyperpolarized mid-inactivation potential (V_h) of I_{Na} by 2.7 mV and 6.7 mV in sham and epileptic animals, respectively (Figure 3, Table 2). Those shifts in steady-state inactivation would theoretically reduce I_{Na} amplitude by 12% and 18% in sham and epileptic animals when cardiomyocytes are sitting around their natural resting membrane potential of −80 mV and may contribute to a reduction in cell excitability.
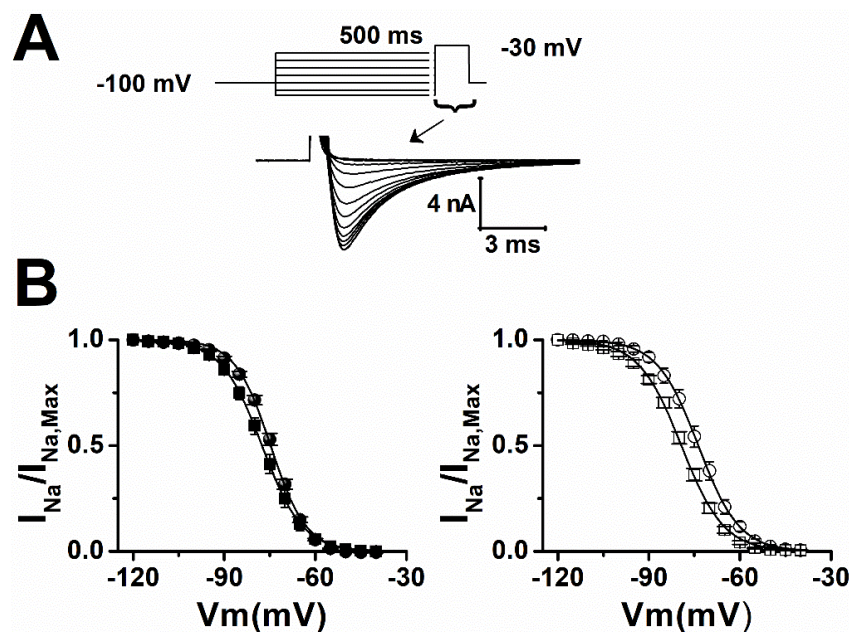

Figure 3. LTG hyperpolarized I_{Na} steady state-inactivation. (**A**) Representative I_{Na} inactivation recording obtained during a 15 ms test pulse to −30 mV following a series of 500 ms conditioning potentials from −120 to −40 mV in 5 mV increments (top). (**B**) Steady-state inactivation curves for sham (filled symbol) and epileptic (open symbol) animals in control conditions (circles) and 10 µmol/L of LTG (squares). Data points (±SEM) were fitted using a Boltzmann function (solid line). Number of animals: 3/group (ctrl and LTG). Number of cells: Sham (ctrl, LTG):15, 11; Epileptic (ctrl, LTG): 12, 19.

Table 2. Na^+ channel inactivation parameters for control conditions and during exposure to 10 µmol/L of LTG. Tukey test using one-way ANOVA (ctrl vs. LTG), * indicates $p < 0.05$, ** $p < 0.01$.

Sham	V_h (mV)	Slope
ctrl	−74.5 ± 0.6	5.9 ± 0.2
LTG	−77.2 ± 1.2 *	6.5 ± 0.2 *
epileptic		
ctrl	−73.3 ± 1.4	6.5 ± 0.3
LTG	−80 ± 1 **	7 ± 0.2

I_{Na} recovery from inactivation plays an important role in regulating the minimal time needed between successive action potentials (refractory period). Using standard recovery protocols (Figure 4A), we found that I_{Na} recovery was best described by a sum of two exponentials. Fitting data to a two-exponential function showed that epilepsy alone delayed recovery by increasing the slow recovery time constant by 20%. LTG only slightly slowed recovery of I_{Na} in sham and epilepsy cardiomyocytes (Figure 4B, Table 3).
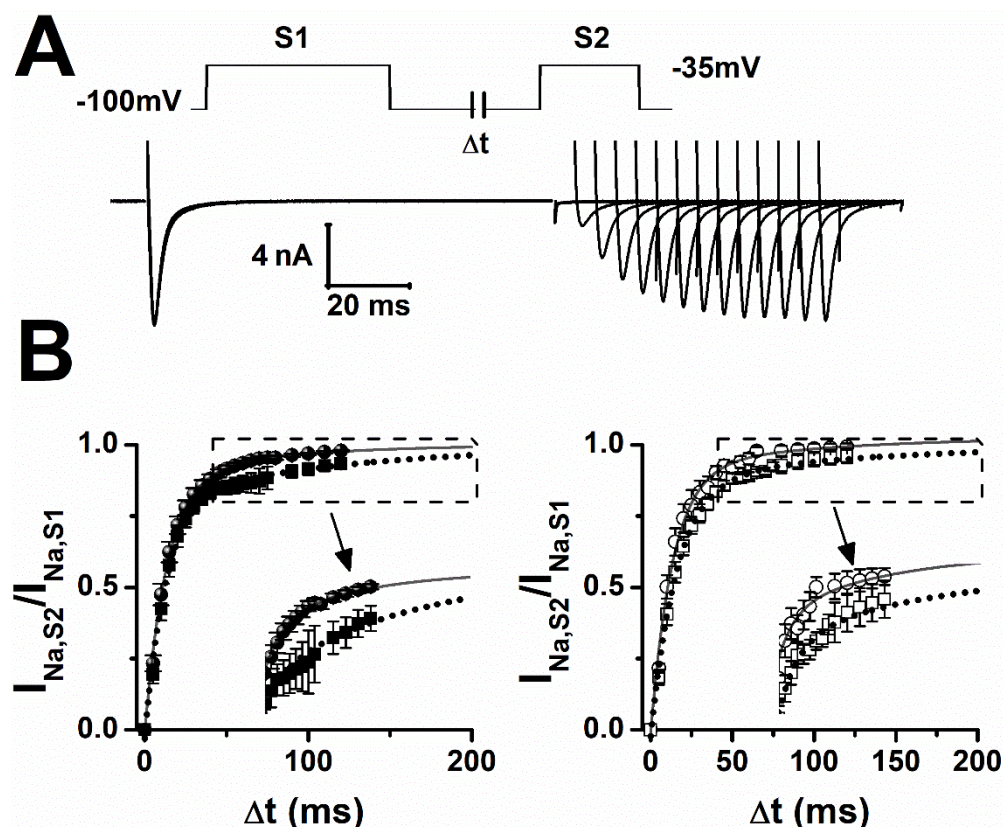
Figure 4. LTG slows I_{Na} recovery from inactivation. (**A**) Representative I_{Na} recording during recovery from inactivation. I_{Na} was elicited by two step pulses, S1 (100 ms) and S2 (20 ms) to -35 mV, separated by increasing intervals at the resting membrane potential, in increments of 5 ms. Holding membrane potential was -100 mV. (**B**) Recovery from inactivation curves for sham (filled symbol) and epileptic rats (open symbol) in control (circles), and 10 μmol/L of LTG (squares). Data ($\pm$SEM) were fitted to two exponential functions (solid: control, short-dot line: LTG) to estimate the time constants. Number of animals: 3/group (ctrl and LTG). Number of cells: Sham (ctrl, LTG):19, 9; Epileptic (ctrl, LTG): 9, 15.

Table 3. Time constant values of I_{Na} recovery from inactivation. The relative weights for fast and slow components are indicated by I_f and I_s, respectively. Tukey test using one-way ANOVA (ctrl vs. LTG), * indicates $p < 0.05$, ** indicates $p < 0.01$, and *** indicates $p < 0.001$. § indicates $p < 0.05$ (sham vs. epileptic).

Sham	τ_f (ms)	I_f (%)	τ_s (ms)	I_s (%)
ctrl	15 ± 2	92 ± 1	80 ± 2	9 ± 1
LTG	14 ± 1	80 ± 4 **	127 ± 3 ***	20 ± 1 **
epileptic				
ctrl	11 ± 1	87 ± 4	97 ± 8 §	13 ± 4 §
LTG	17 ± 2 *	88 ± 1 §	130 ± 2 ***	12 ± 1 §

The refractory period is caused by the time needed for the channels to transit back from the inactivated to the closed state, from which they can re-open. We next tested whether those effects of LTG on I_{Na} recovery translated into a longer refractory period of cardiomyocyte action potentials (Figure 5A,C). In control conditions, the time needed to recover a full amplitude action potential at resting membrane voltages of -80 mV or -100 mV was similar between sham and epileptic animals (Figure 5B,D). LTG (1 μmol/L) increased the total refractory period by $65 \pm 11\%$ and $185 \pm 13\%$ at -80 mV, and by

$106 \pm 17\%$ and $173 \pm 26\%$ at -100 mV in sham and epileptic animals, respectively. These results indicate that LTG increased the refractory period by a factor of 1.9 for sham and 2.8 for epileptic animals ($p < 0.001$, Tukey test with one-way ANOVA). As previously reported, epileptic rats displayed longer action potentials [20] (Figure S1) at the plateau level in part due to a larger window current (Figure S2). LTG (1 µmol/L) reduced early action potential duration (30% repolarization) by $30.4 \pm 4.2\%$ and $33.5 \pm 4.2\%$ in sham and epileptic animals, respectively. We next evaluated if the effects of LTG on I_{Na} late current could account for the changes in APD. Our measurements using a voltage ramp protocol showed that epilepsy increased I_{NaL} by $26 \pm 9.2\%$, from -1.5 ± 0.2 to -1.9 ± 0.1 pA/pF (Figure 6A), as we previously reported [20,21]. Following application of 10µmol/L of LTG, I_{NaL} amplitude was reduced from -1.5 ± 0.2 to -1.4 ± 0.2 pA/pF and from -1.9 ± 0.1 to -0.6 ± 0.1 pA/pF in sham and epileptic animals, respectively (Figure 6B). This reduction in I_{NaL} represents a block of $6.7 \pm 4.3\%$ in sham and $66.7 \pm 5.8\%$ during epilepsy. LTG at 10 µmol/L decreased the window current calculated from the overlap of the activation and steady-state inactivation of I_{Na} by 9.5% and 91.3% in sham and epileptic animals, respectively (Figure S2). These values are close to those found experimentally with our I_{NaL} measurements. Overall, our data show a strong contribution of I_{NaL} blockade to modulation of APD by LTG.
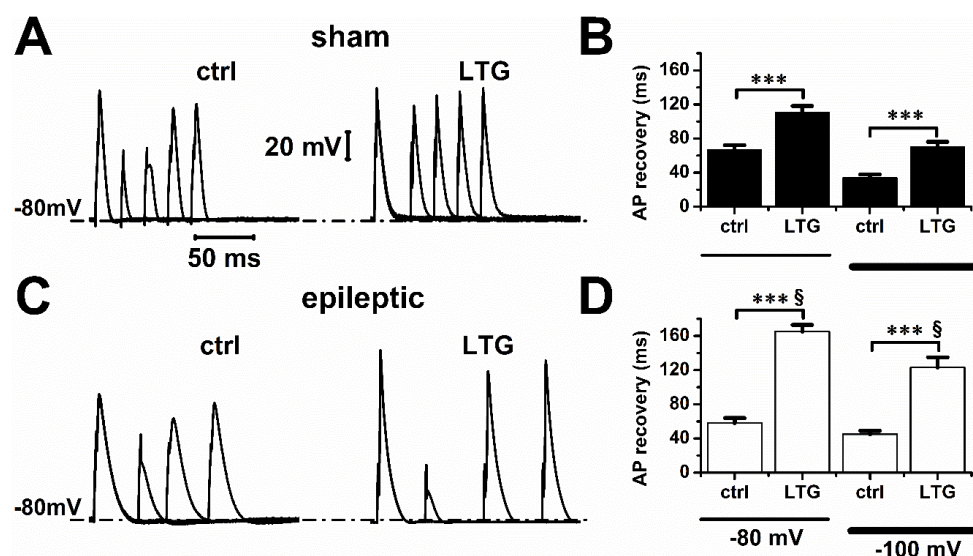

Figure 5. LTG prolonged cardiac action potential refractory period. (**A**,**C**) Representative action potential recordings from sham and epileptic rats in control (ctrl) and in presence of 1 µmol/L of LTG. Cardiomyocytes were held at membrane potentials of -80 or -100 mV and stimulated at a pacing cycle length of 2 ms (sham) and 10 ms (epileptic) for control experiments, and 5 ms (sham) and 50 ms (epileptic) to 1 µmol/L of LTG. For simplicity, only representative records of cells held at -80 mV are shown in the figure. However, as indicated above, the recordings were also performed on the same cell at -100 mV. (**B**,**D**) Action potential (AP) recovery time was measured as the time needed to recover a full amplitude action potential. Each bar represents the average value ($\pm$SEM). Tukey test using one-way ANOVA (ctrl vs. LTG), *** indicates $p < 0.001$, and [§] indicates $p < 0.001$ (sham vs. epileptic). Number of animals: 3/group (ctrl and LTG). Number of cells: Sham (ctrl, LTG):14, 14; Epileptic (ctrl, LTG): 14, 12.
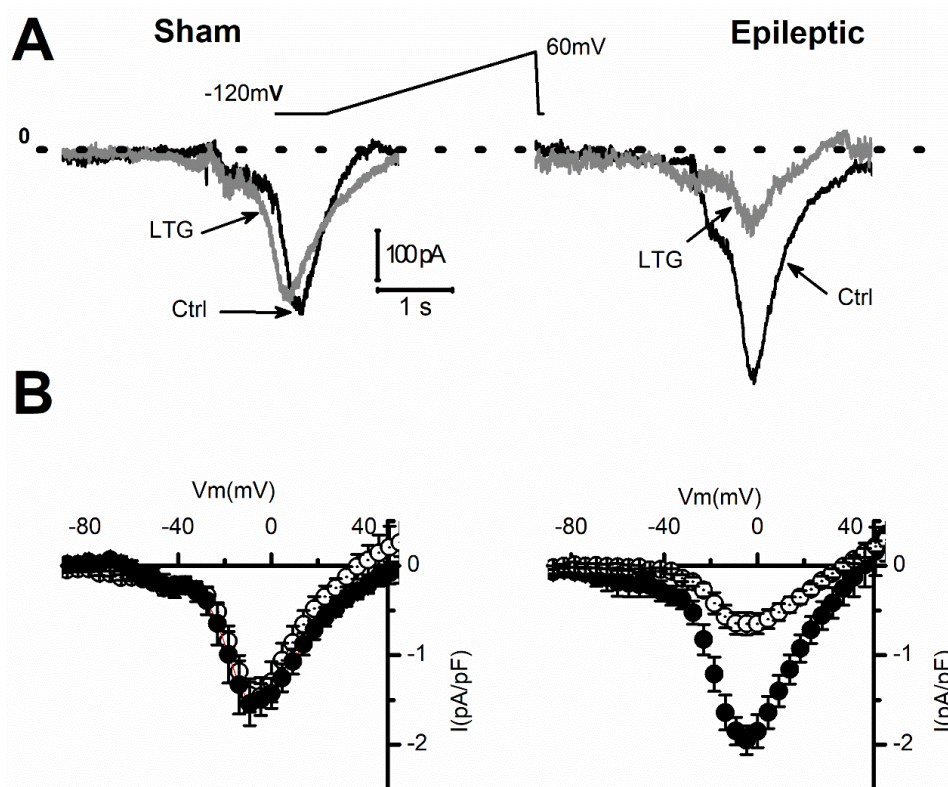
Figure 6. LTG blocked I_{NaL} current in cardiomyocytes from epileptic animals but had no effect in sham rats. (**A**) Representative I_{NaL} recordings from sham and epileptic rat cardiomyocytes in control conditions (ctrl, black) and in presence of 10 μmol/L/L of Lamotrigine (LTG, gray). Currents were elicited by a voltage ramp protocol from −120 to 60 mV with a 0.04 mV/ms rate. (**B**) IV-curves showing the average of current density values for sham (left) and epileptic animals (right) in control conditions (filled circles) and to 10 μmol/L/L of LTG (empty circles). Number of animals: 3/group (ctrl and LTG). Number of cells: Sham (ctrl, LTG):12, 12; Epileptic (ctrl, LTG): 14, 16.

3. Discussion

The Na$^+$ channel family consists of 10 pore-forming α-subunits associated with auxiliary β-subunits identified as $β_1$ through $β_4$ [22]. Among them, tetrodotoxin (TTX)-sensitive voltage-gated channels Na$_V$1.1, Na$_V$1.2, Na$_V$1.3 and Na$_V$1.6 are the most abundantly expressed in the brain, while the TTX-resistant Na$_V$1.5 is considered the cardiac isoform [23]. Overexpression of Na$_V$1.1 and Na$_V$1.3 within the brain has been reported in non-hereditary forms of epilepsy [24,25]. In a previous study, we demonstrated that epilepsy also enhances expression of TTX-sensitive channels (among them, Na$_V$1.1) within the rat cardiac ventricle.

In the heart, sodium channels contribute to conduction and cellular excitability by modulating the voltage threshold, the rising phase, and the duration of action potentials. Although the bulk of sodium current is carried by the cardiac isoform Na$_V$1.5, we previously showed that tetrodotoxin TTX-sensitive channels contribute to I_{Na} and I_{NaL} [21,26,27] This contribution increased during epilepsy. We previously reported contributions of ≈19% and ≈35% to I_{NaL} for epileptic rats. Our data (Figure 1) show that blockade of I_{Na} is more important in cardiomyocytes from epileptic animals. Therefore, our observation of a saturating block by LTG is most likely linked to blockade of neuronal channel isoforms overexpressed during epilepsy and contributing to I_{Na}. Those data are consistent with our previous RT-PCR and Western blot analyses showing that cDNA and protein expression of neuronal sodium channels, especially Na$_V$1.1, is enhanced in cardiac ventricles of epileptic animals [20].

However, we were surprised by the amplitude of the block by LTG during epilepsy. Based on our previous results showing that 35% of peak I_{Na} is generated by TTX-sensitive

channels in epileptic animals, we were expecting a proportional level of I_{Na} block by LTG. The 61% block shown on the peak I_{Na}-I/V curve and the plateau at 53% block on the dose–response curve for epileptic animals (Figure 2) indicates that some $Na_V1.5$ channels might also have been blocked but with a lower affinity, or part of the blockade is due to the inactivation kinetics of I_{Na}.

The modulated receptor hypothesis of Hille [28] may explain blockade of neuronal sodium channels by LTG. Under this model, LTG binds to open channels and stabilizes inactivation in a higher affinity block [6,29–32]. This mechanism is generally thought to be responsible for the use-dependent block of I_{Na} by local anesthetics such as lidocaine [33]. It was proposed to explain the antiepileptic effect of LTG by accumulation of I_{Na} block in the inactivated states during rapid firing in hippocampus [1]. Such a mechanism is consistent with our data showing minimal alterations of steady-state activation in both sham and epileptic animals but a significant hyperpolarization of I_{Na} mid-inactivation potential during epilepsy (Figure 3), as previously reported [2]. The higher affinity block in the inactivated state may also explain the slower recovery of I_{Na} in both sham and epileptic animals. Given that our pulse protocol to measure I_{Na} was 25 ms, nNavs had more time to inactivate, and this may have increased blockade by LTG at lower concentrations. Therefore, the saturating effect of LTG block can be explained by a low-affinity blockade of cardiac $Na_V1.5$ channels and a high-affinity blockade of nNavs overexpressed during epilepsy.

A key difference between neuronal and cardiac action potentials is their duration (APD). In neurons from the central nervous system, APD is between 1 and 10 ms [34] as opposed to cardiac ventricular APD, which will vary from 20–80 ms in rodents and up to 450 ms in humans [35]. Therefore, any neuronal sodium channel isoform sensitive to LTG will have a much longer inactivation time in the heart, and this will promote a more important block of I_{Na}. Potentiation of I_{Na} blockade may significantly reduce conduction and potentiate ventricular bradycardia by prolonging the refractory period and reducing APD, as observed during our action potential measurements in cardiomyocytes from epileptic animals.

Interestingly, the reduction in APD occurs at 30% and 50% repolarization (Figure S1), which is the region of major I_{NaL} involvement and is more important in epileptic animal vs. sham. In agreement, we found a larger reduction in I_{NaL} during epilepsy. Prolongation of the refractory period is anti-arrhythmic in cases where heart rate is rapid, such as in tachycardia and polymorphic VT. In those type of arrythmias, the beneficial effect comes from slowing the accelerated heart rate or reducing dispersion of electrical repolarization within the ventricle. However, in normal settings, an increase in I_{Na} refractory period could prevent subsequent beats from occurring normally and slow cardiac rhythm to rates that cause bradycardia. In those conditions, slowing recovery of I_{Na} may, therefore, potentiate cardiac arrhythmias. This represents a potential mechanism that may explain the clinical observations of bradycardia and conduction problems in patients treated with LTG.

Late sodium current contributes to AP repolarization plateau, and its enhancement causes a longer QT interval, which triggers arrhythmias. Our results show that epilepsy increased I_{NaL} amplitude by 27%, a value close to what we already reported [20]. Interestingly, LTG at therapeutic concentration (10 µmol/L) reduced I_{NaL} by 66.7 ± 5.8% only in epileptic animals (Figure 6), further suggesting a significant contribution of LTG-sensitive nNavs during epilepsy. Our results show that epilepsy increased blockade of I_{NaL} by LTG by a factor of 10. I_{NaL} inhibition could have benefits against pathologies such as drug-induced or hereditary long QT syndrome [35] by reducing the duration of the ventricular AP duration. We previously reported that epilepsy prolonged ventricular APD by increasing I_{NaL}. Our results suggest that LTG may prevent or reduce QT prolongation in epileptic individuals. However, this protective effect may be lost when combined with blockade of the I_{Na} peak (61%). Indeed, a reduction in peak I_{Na} will impact the early phase 1 of the AP by disturbing the balance between I_{Na} and the transient outward potassium current (I_{to}), especially in the epicardial layer of the ventricle. The reduction in I_{Na} amplitude will potentiate early repolarization by I_{to}. Adding the APD shortening effect of weaker

I_{NaL} is likely to further promote early repolarization, a hallmark of BrS. In regions, such as the epicardium of the right ventricle, where I_{to} is most prominent, repolarization will occur rapidly, while the inner part of the ventricle will remain fully depolarized [36]. This dispersion of repolarization within the cardiac ventricle can trigger shunt currents from the still depolarized areas to the fully repolarized regions. Consequently, the fully repolarized regions of the epicardium may re-excite prematurely, thus creating a substrate for re-entrant arrhythmias. This may in part explain the observations of BrS arrhythmias in epileptic patients treated with LTG.

Overall, our data demonstrate that LTG, by virtue of its effect on I_{Na}, may cause a reduction in cardiac conduction speed, excitability and APD. Those effects are consistent with clinical observations of QRS widening [18,37–39] during LTG overdose and BrS phenotypes [11,12,36,40,41] in epileptic patients. Moreover, because of the enhanced expression of nNavs sensitive to LTG during epilepsy, our data may in part explain why cardiac disturbances seem relatively benign during overdose in patients treated for depression-related illness but may become serious and potentially deadly for epileptic patients. Our study thus provides a basic framework to explain the increased risk of cardiac arrhythmias seen in epileptic patients under treatment with LTG.

4. Methods

4.1. Animal Model and Cell Dissociation

Epilepsy was induced in rats by subcutaneous injection of Kainic acid (KA, Hello Bio Inc., Princeton, NJ, USA) as previously described [20]. Briefly, adult Sprague Dawley rats (~250–275 g) were injected twice with 8 mg/kg of KA, with a 1.5 to 2 h interval between injections, to induce seizures. The status epilepticus was stopped by intraperitoneal (IP) injection of 25 mg/kg of diazepam (Valium, Rexall Pharmacy Group Ltd., Toronto, ON, Canada) 2 h after KA. Animals were constantly monitored for 36–40 days after induction of epilepsy. Only animals showing chronic seizure behavior consisting of rearing and falling corresponding to stages 4 and 5 on the Racine scale over the course of 36 day were used in this study [42]. Sham animals received diazepam and saline in lieu of KA. Animals were housed 1 per cage on a 14 h/10 h light/dark cycle with free access to tap water and food. All animals were used between 36 and 40 days after treatment. Left ventricular cardiomyocytes from adult rats were isolated by enzymatic dissociation as we previously described [26,43]. Animals were euthanized by exsanguination. Briefly, rats were injected intraperitoneally with 500 U/kg of Sodium Heparin (Sandoz Canada Inc., Boucherville, QC, Canada) 20 min prior to sedation with 1-chloro-2,2,2-trifluoroethyl difluoro methyl ether (Isoflurane, USP, Baxter, Simcoe County, ON, Canada). When the animal was fully anesthetized, the chest was opened, and the heart rapidly excised.

4.2. Electrophysiology

I_{Na} was recorded from ventricular cardiomyocytes at room temperature with the patch clamp technique in whole cell configuration using an Axopatch 200B amplifier (Molecular Devices, Sunnyvale, CA, USA). Analysis was performed using the Clampex 10.7 analysis software. Recordings were acquired at 10 kHz and filtered to 5 kHz (lowpass Bessel filter). Whole cell capacitance and series resistance compensation (85%) were optimized to reduce the capacitive artifact and minimize voltage clamp error.

Cells from both sham and epileptic animals were incubated for 10 min with various concentrations of LTG and perfused constantly during patch clamp measurements. I_{Na} recordings took around 20 min. The quality of the giga-seal after the 20 min was, in most cases, not good enough to perform LTG washout and attempt to record the current again.

For action potential (AP) measurements, membrane potential was kept at either -100 mV or -80 mV in current clamp mode (I = 0). Action potentials were triggered by 1 ms pulses of threshold current applied at a frequency of 20 Hz where mentioned. It is important to note that in the LTG experiments, it was necessary to perform the AP

measurements with 1 μmol/L instead of 10 μmol/L, because the AP was not triggered in the presence of 10 μmol/L, which introduced substantial variability in the results.

The extracellular recording solution for I_{Na} measurements contained (in mmol/L): 117.5 Choline-Cl, 10 NaOH, 2.8 Na-Acetate, 4 KOH, 1 $CaCl_2$, 1.5 $MgCl_2$, 20 HEPES, 1 $CoCl_2$, 5 TEA, 2 4-AP, 5 $BaCl_2$, 10 Glucose. The pH and osmolarity were adjusted to 7.4 (with NaOH) and 295–300 mOsm (sucrose). Pipette solution contained (in mmol/L): 10 NaOH, 5 NaCl, 5 CsF, 2 $MgCl_2$, 10 EGTA, 20 HEPES, 120 Cesium-Aspartate, 0.5 GTP, 3 Creatine Phosphate, 2 ATP-Mg. The pH was adjusted with CsOH to 7.3 and osmolarity to 295–300 mOsm.

The solutions for I_{NaL} recordings (in mmol/L) were: 10 NaOH, 5 NaCl, 5 KOH, 4 $MgCl_2$, 10 EGTA, 20 HEPES, 120 CsOH, and 4 Na_2-ATP for pipette solution. The pH was adjusted to 7.3 with CsOH and osmolarity to 290–300 mOsmol/L. Extracellular solution contained: 125 NaCl, 10 NaOH, 2.8 Na-Acetate, 4 KOH, 1 $CaCl_2$, 1.5 $MgCl_2$, 20 HEPES, 1 $CoCl_2$, 5 TEA, 2 4-AP, 5 $BaCl_2$, 10 Glucose. The pH and osmolarity were adjusted to 7.4 (with NaOH) and 295–300 mOsmol/L (sucrose).

For AP measurements, the cardiomyocyte bath solution contained (in mmol/L): 126 NaCl, 5.4 KCl, 2 $CaCl_2$, 1 $MgCl_2$, 20 HEPES, 11 Glucose; and for pipette solution: 90 K-aspartate, 30 KCl, 10 NaCl, 5.5 Glucose, 1 $MgCl_2$, 10 EGTA, 4 Na-ATP, 20 HEPES. Extracellular and intracellular solution pH was adjusted to 7.4 (NaOH) and 7.2 (KOH), respectively.

Recording pipettes were pulled from 1.5 mm O.D., 1.16 mm I.D. capillary glass (PGT150T-7.5 Harvard Apparatus) and had resistance between 1 and 3 MΩ.

4.3. Materials

Lamotrigine (LTG, ApexBio LLC Technology, Houston, TX, USA) was dissolved in DMSO to make a stock solution of 0.3 mol/L, from which we diluted in extracellular solution to reach the final concentrations. DMSO in LTG extracellular solutions never exceeded 0.2%. No DMSO effects on I_{Na} were observed at this maximum concentration.

4.4. Data Analysis

Figures were produced and data analysis performed with the pCLAMP program suite software (Molecular Devices, Sunnyvale, CA, USA) and Origin 8.5 (OriginLab, Nothampton, MA, USA).

I_{Na} current voltage relationships were obtained from recordings during 25 ms voltage steps between −70 and 10 mV, in 5 mV increments, from a −100 mV holding potential. Average peak current values were normalized to membrane capacitance (Cm) and plotted against the test voltage to construct the I_{Na} current-voltage curves (pA/pF). Conductance (G_{Na}) was calculated as $G_{Na} = I_{Na}/(Vm − E_{Na})$, where Vm is the membrane potential (mV) and E_{Na} is the sodium reversal potential (mV). Maximum conductance ($G_{Na,Max}$) was obtained from the slope of a linear regression fit to the linear portion of the I/V at voltage more positive than −25 mV.

Steady-state inactivation was measured using a 15 ms test pulse to 30mV following a series of 500 ms conditioning potentials from −120 to −40 mV in 5 mV increments. Inactivation curves were obtained by plotting the ratio of I_{Na} to its maximum value ($I_{Na,Max}$) as a function of the conditioning voltage.

Activation and inactivation data were fitted to a standard Boltzmann distribution function: $Y = \frac{(A_1 − A_2)}{1+[(Vm−E_{Na})/V_{0.5}]} + A_2$, where Y represents the fraction of activated (m) or available (h) channels obtained, respectively, from the ratio of the macroscopic conductance ($G_{Na}/G_{Na,Max}$) or the sodium current I/I_{Max}. Vm and E_{Na} were defined as before, and $V_{0.5}$ was the mid-potential for activation or inactivation. G_{Na} was obtained from the current–voltage relationship as $G_{Na} = I_{Na}/(Vm − E_{Na})$, and $G_{Na,Max}$ represented the maximal Na^+ conductance. $V_{0.5}$ was the membrane voltage, where the distribution was half-maximal, corresponding to mid-activation or mid-inactivation (V_h) voltages.

Recovery from inactivation was measured using a standard double-pulse protocol while holding cells to membrane potentials of −100 mV. I_{Na} was elicited by two-step pulses

S1 (100 ms) and S2 (20 ms) to −35 mV, separated by increasing intervals at the holding membrane potential, in increments of 5 ms. Recovery from inactivation was obtained by plotting the ratio of I_{Na} amplitudes (S2/S1) as a function of the time interval Δt. Time constants (τ) were calculated from a sum of two exponential functions fit to the ratio of $I_{Na,S2}/I_{Na,S1}$: $\frac{I_{Na,S2}}{I_{Na,S1}} = I_0 + I_s * exp\left(\frac{-t}{\tau s}\right) + I_f * exp\left(\frac{-t}{\tau f}\right)$, where I_s and I_f and τ_s and τ_f represent the fraction of current and time constants for the slow and fast components of I_{Na} recovery, respectively.

I_{NaL} current was induced by applying a depolarizing voltage ramp protocol, from −120 mV to +60 mV, at a 0.04 V/s rate. This protocol inactivated the peak sodium current. Digital subtraction of traces in the absence and presence of 10 µmol/L/L of tetrodotoxin (TTX) yielded the I_{NaL}.

Dose–response curves. The values of the maximum current density amplitude obtained for each drug concentration were divided by the average of the maximum current density amplitude obtained under control conditions, then the data were plotted as a function of *LTG* concentration tested and fitted to monophasic (sham) or biphasic response (epileptic) Hill absorption isotherm:

$$\frac{I_{Na}}{I_{Na,Max}} = \frac{1}{1 + \left(\frac{[LTG]}{IC_{50,LTGr}}\right)} \text{(sham)}$$

$$\frac{I_{Na}}{I_{Na,Max}} = \left\{ \frac{f_{LTGrs}}{1 + \left(\frac{[LTG]}{IC_{50,LTGs}}\right)} + \frac{(1 - f_{LTGs})}{1 + \left(\frac{[LTG]}{IC_{50,LTGr}}\right)} \right\} \text{(epileptic)}$$

Parameters f_{LTG} and $IC_{50,LTG}$ represent the fraction blocked by *LTG* and half maximal blocking concentration, respectively. The half blocking concentration of *LTG* was initially determined by fitting the data from sham animals (IC_{50LTGr}) and used as seed value to fit the epileptic animal data to the sum of two Langmuir isotherms, keeping the assumption of a 1:1 binding to all receptors.

4.5. Statistics

Experimental data points are presented as data $\pm$ SEM, and number of cells is indicated in each Figure. Statistics were performed using the Tukey test comparing groups with one-way ANOVA.

Abbreviations

Meaning	Abbreviation
Lamotrigine	LTG
Voltage-gated sodium channels	VGSC
US Food and Drug Administration	FDA
Brugada syndrome	BrS
Cardiac sodium current	I_{Na}
Late sodium current	I_{NaL}
Electrocardiogram	ECG
Voltage-gated neuronal sodium channels	nNa_Vs
Animal Research: Reporting In-Vivo Experiments	ARRIVE
Kainic Acid	KA
Intraperitoneal	IP
Action Potential	AP
Dimethyl Sulfoxide	DMSO
Standard Error Mean	SEM
Analysis of Variance	ANOVA
Tetrodotoxin	TTX
Action Potential Duration	APD

References

1. Xie, X.; Lancaster, B.; Peakman, T.; Garthwaite, J. Interaction of the antiepileptic drug lamotrigine with recombinant rat brain type IIA Na+ channels and with native Na+ channels in rat hippocampal neurones. *Pfluegers Arch. Eur. J. Physiol.* **1995**, *430*, 437–446. [CrossRef] [PubMed]
2. Kuo, C.C.; Lu, L. Characterization of lamotrigine inhibition of Na+ channels in rat hippocampal neurones. *Br. J. Pharmacol.* **1997**, *121*, 1231–1238. [CrossRef] [PubMed]
3. Huang, C.-W.; Huang, C.-C.; Liu, Y.-C.; Wu, S.-N. Inhibitory Effect of Lamotrigine on A-type Potassium Current in Hippocampal Neuron-Derived H19-7 Cells. *Epilepsia* **2004**, *45*, 729–736. [CrossRef] [PubMed]
4. Fleurat, M.; Smollin, C. Case Files of the University of California San Francisco Medical Toxicology Fellowship: Lamotrigine Toxicity. *J. Med. Toxicol.* **2012**, *8*, 52–58. [CrossRef] [PubMed]
5. Lang, D.G.; Wang, C.M.; Cooper, B.R. Lamotrigine, phenytoin and carbamazepine interactions on the sodium current present in N4TG1 mouse neuroblastoma cells. *J. Pharmacol. Exp. Ther.* **1993**, *266*, 829–835. [PubMed]
6. Cronin, N.B.; O'Reilly, A.; Duclohier, H.; Wallace, B.A. Binding of the Anticonvulsant Drug Lamotrigine and the Neurotoxin Batrachotoxin to Voltage-gated Sodium Channels Induces Conformational Changes Associated with Block and Steady-state Activation. *J. Biol. Chem.* **2003**, *278*, 10675–10682. [CrossRef]
7. Nakatani, Y.; Masuko, H.; Amano, T. The Effect of Lamotrigine on Nav1.4 Voltage-Gated Sodium Channels. *J. Pharmacol. Sci.* **2013**, *123*, 203–206. [CrossRef]
8. Bendtsen, L.; Zakrzewska, J.M.; Abbott, J.; Braschinsky, M.; Di Stefano, G.; Donnet, A.; Eide, P.K.; Leal, P.R.L.; Maarbjerg, S.; May, A.; et al. European Academy of Neurology guideline on trigeminal neuralgia. *Eur. J. Neurol.* **2019**, *26*, 831–849. [CrossRef]
9. Jansen, A.C.; Andermann, E. Progressive Myoclonus Epilepsy, Lafora Type. In *GeneReviews®*; Adam, M.P., Ardinger, H.H., Pagon, R.A., Wallace, S.E., Bean, L.J., Mirzaa, G., Amemiya, A., Eds.; University of Washington: Seattle, WA, USA, 1993. Available online: http://www.ncbi.nlm.nih.gov/books/NBK1389/ (accessed on 27 September 2021).
10. Brigo, F.; Igwe, S.C.; Lattanzi, S. Ethosuximide, Sodium Valproate or Lamotrigine for Absence Seizures in Children and Adolescents. *Cochrane Database Syst. Rev.* **2021**, CD003032. Available online: https://www.cochranelibrary.com/cdsr/doi/10.1002/14651858.CD003032.pub5/epdf/full (accessed on 27 September 2022).
11. Strimel, W.J.; Woodruff, A.; Cheung, P.; Kirmani, B.F.; Stephen Huang, S.K. Brugada-like electrocardiographic pattern induced by lamotrigine toxicity. *Clin. Neuropharmacol.* **2010**, *33*, 265–267. [CrossRef]
12. Rodrigues, R.; Amador, P.; Rassi, L.; Seixo, F.; Parreira, L.; Fonseca, N.; Soares, L. Padrão de Brugada em doente medicada com lamotrigina. *Rev. Port. Cardiol.* **2013**, *32*, 807–810. [CrossRef] [PubMed]
13. Leong, K.M.W.; Seligman, H.; Varnava, A.M. Proarrhythmogenic effects of lamotrigine during ajmaline testing for Brugada syndrome. *Heart Case Rep.* **2017**, *3*, 167–171. [CrossRef] [PubMed]
14. Banfi, P.; Coll, M.; Oliva, A.; Alcalde, M.; Striano, P.; Mauri, M.; Princiotta, L.; Campuzano, O.; Versino, M.; Brugada, R. Lamotrigine induced Brugada-pattern in a patient with genetic epilepsy associated with a novel variant in SCN9A. *Gene* **2020**, *754*, 144847. [CrossRef] [PubMed]
15. Herold, T.J.S. Lamotrigine as a possible cause of QRS prolongation in a patient with known seizure disorder. *CJEM* **2006**, *8*, 361–364. [CrossRef]

16. Nogar, J.N.; Minns, A.B.; Savaser, D.J.; Ly, B.T. Severe sodium channel blockade and cardiovascular collapse due to a massive Lamotrigine overdose. *Clin. Toxicol.* **2011**, *49*, 854–857. [CrossRef]

17. Lofton, A.L.; Klein-Schwartz, W. Evaluation of Lamotrigine Toxicity Reported to Poison Centers. *Ann. Pharmacother.* **2004**, *38*, 1811–1815. [CrossRef]

18. Moore, P.W.; Donovan, J.W.; Burkhart, K.K.; Haggerty, D. A case series of patients with lamotrigine toxicity at one center from 2003 to 2012. *Clin. Toxicol.* **2013**, *51*, 545–549. [CrossRef]

19. French, J.A.; Perucca, E.; Sander, J.W.; Bergfeldt, L.; Baulac, M.; Auerbach, D.S.; Keezer, M.; Thijs, R.D.; Devinsky, O.; Vossler, D.G.; et al. FDA safety warning on the cardiac effects of lamotrigine: An advisory from the Ad Hoc ILAE/AES Task Force. *Epilepsia Open* **2021**, *6*, 45–48. [CrossRef] [PubMed]

20. Biet, M.; Morin, N.; Lessard-Beaudoin, M.; Graham, R.K.; Duss, S.; Gagne, J.; Sanon, N.T.; Carmant, L.; Dumaine, R. Prolongation of Action Potential Duration and QT Interval during Epilepsy Linked to Increased Contribution of Neuronal Sodium Channels to Cardiac Late Na+ Current: A Potential Mechanism for Sudden Death in Epilepsy. *Circ. Arrhythm. Electrophysiol.* **2015**, *8*, 912–920. [CrossRef]

21. Biet, M.; Barajas-Martinez, H.; Ton, A.T.; Delabre, J.F.; Morin, N.; Dumaine, R. About half of the late sodium current in cardiac myocytes from dog ventricle is due to non-cardiac-type Na(+) channels. *J. Mol. Cell Cardiol.* **2012**, *53*, 593–598. [CrossRef]

22. Catterall, W.A.; Perez-Reyes, E.; Snutch, T.P.; Striessnig, J. International Union of Pharmacology. XLVIII. Nomenclature and structure-function relationships of voltage-gated calcium channels. *Pharmacol. Rev.* **2005**, *57*, 411–425. [CrossRef] [PubMed]

23. Kwong, K.; Carr, M.J. Voltage-gated sodium channels. *Curr. Opin. Pharmacol.* **2015**, *22*, 131–139. [CrossRef] [PubMed]

24. Guo, F.; Xu, X.; Cai, J.; Hu, H.; Sun, W.; He, G.; Shao, D.; Wang, L.; Chen, T.; Shaw, C.; et al. The up-regulation of voltage-gated sodium channels subtypes coincides with an increased sodium current in hippocampal neuronal culture model. *Neurochem. Int.* **2013**, *62*, 287–295. [CrossRef] [PubMed]

25. Guo, F.; Yu, N.; Cai, J.Q.; Quinn, T.; Zong, Z.H.; Zeng, Y.J.; Hao, L.Y. Voltage-gated sodium channel Nav1.1, Nav1.3 and beta1 subunit were up-regulated in the hippocampus of spontaneously epileptic rat. *Brain Res. Bull.* **2008**, *75*, 179–187. [CrossRef]

26. Haufe, V.; Cordeiro, J.; Zimmer, T.; Wu, Y.; Schiccitano, S.; Benndorf, K.; Dumaine, R. Contribution of neuronal sodium channels to the cardiac fast sodium current is greater in dog heart Purkinje fibers than in ventricles. *Cardiovasc Res.* **2005**, *65*, 117–127. [CrossRef]

27. Haufe, V.; Chamberland, C.; Dumaine, R. The promiscuous nature of the cardiac sodium current. *J. Mol. Cell Cardiol.* **2007**, *42*, 469–477. [CrossRef]

28. Hille, B. Local anesthetics: Hydrophilic and hydrophobic pathways for the drug-receptor reaction. *J. Gen. Physiol.* **1977**, *69*, 497–515. [CrossRef]

29. Qiao, X.; Sun, G.; Clare, J.J.; Werkman, T.R.; Wadman, W.J. Properties of human brain sodium channel α-subunits expressed in HEK293 cells and their modulation by carbamazepine, phenytoin and lamotrigine: Properties of brain Na channel α-subunits. *Br. J. Pharmacol.* **2014**, *171*, 1054–1067. [CrossRef]

30. Tikhonov, D.B.; Zhorov, B.S. Mechanism of sodium channel block by local anesthetics, antiarrhythmics, and anticonvulsants. *J. Gen. Physiol.* **2017**, *149*, 465–481. [CrossRef]

31. Liu, G.; Yarov-Yarovoy, V.; Nobbs, M.; Clare, J.J.; Scheuer, T.; Catterall, W.A. Differential interactions of lamotrigine and related drugs with transmembrane segment IVS6 of voltage-gated sodium channels. *Neuropharmacology* **2003**, *44*, 413–422. [CrossRef]

32. Yarov-Yarovoy, V.; Brown, J.; Sharp, E.M.; Clare, J.J.; Scheuer, T.; Catterall, W.A. Molecular determinants of voltage-dependent gating and binding of pore-blocking drugs in transmembrane segment IIIS6 of the Na(+) channel alpha subunit. *J. Biol. Chem.* **2001**, *276*, 20–27. [CrossRef] [PubMed]

33. Bean, B.P.; Cohen, C.J.; Tsien, R.W. Lidocaine block of cardiac sodium channels. *J. Gen. Physiol.* **1983**, *81*, 613–642. [CrossRef] [PubMed]

34. Bean, B.P. The action potential in mammalian central neurons. *Nat. Rev. Neurosci.* **2007**, *8*, 451–465. [CrossRef]

35. Antzelevitch, C.; Dumaine, R. Electrical heterogeneity in the heart: Physiological, pharmacological and clinical implications. In *Handbook of Physiology. Section 2 the Cardiovascular System*; Page, E., Fozzard, H.A., Solaro, R.J., Eds.; Oxford University Press: New York, NY, USA, 2001; pp. 654–692. Available online: http://www.comprehensivephysiology.com/WileyCDA/CompPhysArticle/refId-cp020117.html (accessed on 27 September 2021).

36. Antzelevitch, C.; Brugada, P.; Brugada, J.; Brugada, R. *The Brugada Syndrome: From Bench to Bedside*; Blackwell Futura: Oxford, UK, 2005.

37. Chavez, P.; Casso Dominguez, A.; Herzog, E. Evolving Electrocardiographic Changes in Lamotrigine Overdose: A Case Report and Literature Review. *Cardiovasc Toxicol.* **2015**, *15*, 394–398. [CrossRef] [PubMed]

38. Wood, K.E.; Palmer, K.L.; Krasowski, M.D. Correlation of elevated lamotrigine and levetiracetam serum/plasma levels with toxicity: A long-term retrospective review at an academic medical center. *Toxicol. Rep.* **2021**, *8*, 1592–1598. [CrossRef] [PubMed]

39. Alyahya, B.; Friesen, M.; Nauche, B.; Laliberté, M. Acute lamotrigine overdose: A systematic review of published adult and pediatric cases. *Clin. Toxicol.* **2018**, *56*, 81–89. [CrossRef]

40. Hong, K.; Vatta, M.; Poungvarin, N.; Oliva, A.; Berruero, A.; Pinero, C.; Brugada, J.; Towbin, J.A.; Dumaine, R.; Brugada, P.; et al. SUDS and Brugada Syndrome Linked by the Same SCN5A Mutation. *Circulation* **2002**, *106* (Suppl. 19), II-61.

41. Abdelghani, M.S.; Chapra, A.; Asaad, N.; Hayat, S.A. Epilepsy and Brugada Syndrome: Association or Uncommon Presentation? *Heart Views Off. J. Gulf. Heart Assoc.* **2020**, *21*, 114–117. [CrossRef]

42. Racine, R.J.; Gartner, J.G.; McIntyre Burnham, W. Epileptiform activity and neural plasticity in limbic structures. *Brain Res.* **1972**, *47*, 262–268. [CrossRef]

43. Barajas-Martinez, H.; Haufe, V.; Chamberland, C.; Roy, M.J.; Fecteau, M.H.; Cordeiro, J.M.; Dumaine, R. Larger dispersion of I_{Na} in female dog ventricle as a mechanism for gender-specific incidence of cardiac arrhythmias. *Cardiovasc. Res.* **2009**, *81*, 82–89. [CrossRef]